Synthesis and structure of the new complex hydride $Li_2BH_4NH_2$†

Philip A. Chater,[a] **William I. F. David**[b] **and Paul A. Anderson***[a]

Received (in Cambridge, UK) 20th July 2007, Accepted 8th October 2007
First published as an Advance Article on the web 23rd October 2007
DOI: 10.1039/b711111h

The structure of the new complex hydride $Li_2BH_4NH_2$, determined through Rietveld analysis of synchrotron X-ray and neutron powder diffraction data, comprises a hexagonal array of discrete $(LiNH_2)_6$ clusters dispersed in a $LiBH_4$ matrix.

The $LiBH_4$–$LiNH_2$ system has been the focus of recent study in the search for new hydrogen storage materials.[1–4] The main phase present in this system, $Li_4BH_4(NH_2)_3$, has a body centred cubic structure with a lattice constant of *ca.* 10.66.[5,6] Pinkerton *et al.*[4] reported that a 1 : 1 ball milled mixture of $LiBH_4$ and $LiNH_2$ formed a new body centred cubic phase with a lattice constant of 10.4 Å. However, Noritake *et al.*[7] have reported that ball milling a 1 : 1 mixture resulted in a new hexagonal phase with lattice constants of a = 14.49 Å and c = 9.24 Å. We found that this hexagonal phase $Li_2BH_4NH_2$ can also be prepared through the quenching of a melt of a 1 : 1 mixture of $LiBH_4$ and $LiNH_2$ from 190 °C and we report for the first time the structure of this new complex hydride.

$LiBH_4$ and $LiNH_2$ (Sigma-Aldrich, 95% purity) were ground together by hand in a 1 : 1 mole ratio in an argon atmosphere glovebox (O_2 content < 10 ppm) and placed in a quartz tube. The tube was sealed with a Young's tap *via* an Ultra-Torr fitting, removed from the glovebox, connected to an argon gas line and the reactants were then heated in a tube furnace under argon at 1 bar. After heating at 190 °C for 12 h, the sample was quenched through immersing the reaction tube in cold water, re-ground under argon and annealed at 50 °C to improve crystallinity.

Previous unsuccessful attempts to produce single crystals of $Li_4BH_4(NH_2)_3$ from various solvents,[6] and the synthetic conditions used to produce $Li_2BH_4NH_2$ led us to choose the combination of high resolution synchrotron X-ray[8] and neutron powder diffraction[9] measurements that we used previously to solve the structure of $Li_4BH_4(NH_2)_3$.[6] The refined lattice constants at 25 °C were determined as a = 14.48037(28) Å and c = 9.24483(30) Å, giving a hexagonal unit cell volume of 1678.76(8) Å^3. Inspection of the systematic absences of the diffraction pattern indicated that the phase has rhombohedral symmetry. From density and crystallographic arguments the most probable number of formula units per unit cell are 24, 21 or 18. This corresponds to densities of 1.06, 0.93 and 0.80 g cm^{-3}, respectively; all these densities lie between those of the starting materials $LiBH_4$ (0.66 g cm^{-3}) and $LiNH_2$ (1.18 g cm^{-3}).[10] The presence of 24 formula units allows for a body centred cubic arrangement of anions which is seen in the $LiNH_2$ and $Li_4BH_4(NH_2)_3$ crystal structures. However, consideration of the Wyckoff sites shows that without significant disorder a 1 : 1 stoichiometry is not possible, predicting instead a 7 : 9 stoichiometry. Reaction mixtures in the ratios 7 $LiBH_4$: 9 $LiNH_2$ and 9 $LiBH_4$:7 $LiNH_2$ treated in the same way as the 1 : 1 mixture did not give a pure phase.

The choice of 21 formula units gives a density closest to the average of the starting materials ($\frac{1}{2}[0.66 + 1.18] = 0.92$ g cm^{-3}); this is promising because the same method gave an accurate prediction of the correct density for $Li_4BH_4(NH_2)_3$. Only $R3$ and $R3m$ allow for 21 $Li_2BH_4NH_2$ formula units per unit cell without disorder and these both result in linear Li–B–Li–N–Li chains along the c-axis resulting from multiple occupancy of $3a$ $(0,0,z)$ Wyckoff positions. Although the resulting Li–B and Li–N distances could be within the range expected from $LiBH_4$, $LiNH_2$ and $Li_4BH_4(NH_2)_3$, the unlikely geometry of the bonding and the poor fit of all attempted refinements suggested that 21 formula units is improbable. This led us finally to consider 18 formula units which corresponds to a density that is lower than the average of the starting materials. This is plausible as it is not unusual for structures prepared through quenching from elevated temperature to have a lower density than the corresponding stable room temperature forms.[11]

The synchrotron X-ray powder diffraction pattern[8] of $Li_2BH_4NH_2$ is dominated by the scattering of boron and nitrogen, and these were the first atom positions to be investigated using the computer program TOPAS.[12] At this stage all, of the possible space groups, $R3$ (146), $R\bar{3}$ (148), $R32$ (155), $R3m$ (160) and $R\bar{3}m$ (166) were considered.

Starting models were chosen that consisted of 36 generic atoms in all combinations of suitable Wyckoff positions adding up to the correct total for boron and nitrogen; their positions were determined while allowing the scattering powers of the atoms to vary between that of boron and nitrogen. Many of the resultant refinements gave incorrect B : N ratios and extremely poor fits to the diffraction pattern and these atomic arrangements were immediately discarded. Of all the space groups and combinations of Wyckoff site occupations possible, the best fits were found for $R3$ and $R\bar{3}$ with all atoms on general positions and $R3m$ with two $9b$ $(x,-x,z)$ sites and one $18c$ (x,y,z) site occupied. Of these possible space groups, $R3$ has the lowest symmetry with more degrees of freedom than $R\bar{3}$ and $R3m$ which could explain the good fit. The best fits for $R\bar{3}$ and $R3m$ originated from very similar structures. Both are made up of N octahedra centred around the (0,0,0) position, and therefore ($\frac{1}{3}$,$\frac{2}{3}$,$\frac{2}{3}$) and ($\frac{2}{3}$,$\frac{1}{3}$,$\frac{1}{3}$) positions by symmetry, with the B atoms occupying more open positions surrounding these octahedra. The structures differ mainly in the orientation of the N octahedra.[13]

Lithium atoms were then added to these partial structural solutions at appropriate combinations of Wyckoff positions and

---

[a] *School of Chemistry, The University of Birmingham, Edgbaston, Birmingham, UK B15 2TT. E-mail: P.A.Anderson@bham.ac.uk; Fax: +44(0)121 414 4403; Tel: +44(0)121 414 4447*
[b] *ISIS Facility, Rutherford Appleton Laboratory, Chilton, Didcot, Oxon., UK OX11 0QX. E-mail: W.I.F.David@rl.ac.uk; Fax: +44(0)1235 445 383; Tel: +44(0)1235 445 179*

† Electronic supplementary information (ESI) available: a comparison of $R\bar{3}$ and $R3m$ symmetries, a virtual reality image of Fig. 1 and an animated version of Fig. 3. See DOI: 10.1039/b711111h

Table 1 Refined crystallographic data (CCDC 555216): Space group $R\bar{3}$ a = 14.48037(28) Å, c = 9.24483(30) Å. Unit cell volume = 1678.76(8) Å^3

Atom	x/a	y/a	z/c	U_{iso}/Å^2
B	0.6763(5)	0.7520(6)	0.1835(7)	0.0248(20)
H1	0.7363(11)	0.8167(11)	0.2797(14)	0.0447(25)
H2	0.7112(13)	0.7192(13)	0.0933(15)	0.0447(25)
H3	0.6457(11)	0.8057(12)	0.1036(15)	0.0447(25)
H4	0.5982(14)	0.6842(11)	0.2187(14)	0.0447(25)
N	0.1254(4)	0.96896(29)	0.85713(35)	0.0281(12)
H5	0.1015(17)	0.9725(20)	0.7258(19)	0.0745(34)
H6	0.1431(15)	0.9211(14)	0.8288(23)	0.0745(34)
Li1	0.2903(9)	0.0608(9)	0.7816(11)	0.0673(22)
Li2	0.8457(11)	0.8739(12)	0.0747(10)	0.0673(22)

[a] X-ray data: wR_p = 0.0819, R_p = 0.0621. Neutron data (Banks 5 and 6): wR_p = 0.0131 and 0.0107, R_p = 0.0132 and 0.096. χ^2 = 2.264 for 47 variables.

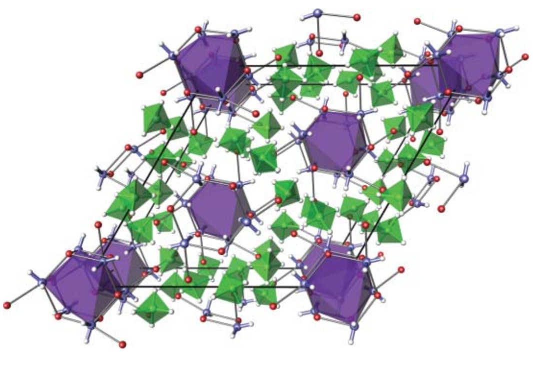

Fig. 1 Crystal structure of $Li_2BH_4NH_2$. H atoms are depicted in white, Li in red, N in blue and BH_4^- as green tetrahedra. Purple N octahedra are added to guide the eye.

"anti-bump" penalties were introduced for short Li–B, Li–N and Li–Li distances (2.0, 1.7 and 2.2 Å respectively). At this point the $R\bar{3}$ structure became favoured, both in the visual and statistical fit.

Rigid bodies for the BH_4^- and NH_2^- ions were introduced at the refined B and N positions for the $R\bar{3}$ structure. Initially BH_4^- was confined to tetrahedral geometry with a bond length of 1.2 Å and the NH_2^- ion to a bond length and angle of 1.0 Å and 105°, respectively. The rotation of these rigid bodies was then refined, followed by refinement of all atomic positions while keeping the rigid body constraints. This model gave a good fit and was transferred to GSAS for full Rietveld refinement using both X-ray and neutron powder diffraction data.[14] Hydrogen displacement parameters were constrained to be the same within each anion (BH_4^- and NH_2^-) and lithium displacement parameters were constrained to be the same on both sites; no further restraints were used. The final joint refinement (Table 1) was essentially similar to that obtained from the X-ray data. The resulting crystal structure is shown in Fig. 1; the corresponding fits to the X-ray and neutron diffraction data are shown in Figs. 2 (a) and (b), respectively.

The bond angles and lengths of the BH_4^- ion refined to values similar to those observed in $LiBH_4$. In contrast, without rigid body constraints, the NH_2^- ion significantly deformed. The refined hydrogen positions in the amide anion may be unreliable because of the relatively low quality of the neutron diffraction data below 1.2 Å resulting from the lack of isotopic enrichment.

The central feature of the $Li_2BH_4NH_2$ structure is the octahedral clusters of six NH_2^- anions. These octahedral NH_2^- clusters are a common structural motif in light metal amides such as $LiNH_2$,[16] $NaNH_2$,[17] $Li_3Na(NH_2)_4$[18] and $Mg(NH_2)_2$,[19] and are also found in the only previously reported amide–borohydride $Li_4BH_4(NH_2)_3$.[5,6] The nitrogen ions in $LiNH_2$ adopt a slightly distorted face centred cubic configuration which can be viewed as edge shared octahedral clusters (Figs. 3a and 4a). In $Li_4BH_4(NH_2)_3$ only one quarter of the edges of the NH_2^- octahedra are shared and the amide framework is penetrated by spiral chains of BH_4^- ions running in three orthogonal directions through this cubic structure (Figs. 3b and 4b). In contrast, for $Li_2BH_4NH_2$ the NH_2^- octahedra are completely isolated in the structure (Figs. 3c and 4c).

The structural progression from $LiNH_2$ through $Li_4BH_4(NH_2)_3$ to $Li_2BH_4NH_2$ may be considered in terms of the ability of $LiBH_4$ at relatively low temperatures to "drill" channels in the $LiNH_2$ to the extent that only small $LiNH_2$ clusters remain in $Li_2BH_4NH_2$. Although $LiNH_2$, $Li_4BH_4(NH_2)_3$ and $Li_2BH_4NH_2$ are insoluble in most common solvents, $LiNH_2$ begins to react with $LiBH_4$ to form $Li_4BH_4(NH_2)_3$ at room temperature and the 1 : 1 mixture from which $Li_2BH_4NH_2$ is formed is entirely molten at 140 °C.

The crystal structure of $Li_2BH_4NH_2$ can be viewed as a mixture of nano-sized clusters of $LiNH_2$ embedded in an $LiBH_4$ matrix. It is easy to see how the metastable $Li_2BH_4NH_2$ may form as it is reasonable to presume that the difference in energy will be small between this nano-mixture of $LiNH_2$ within $LiBH_4$ and the $LiNH_2$:$LiBH_4$ melt. The presence of isolated NH_2^- octahedra in the $Li_2BH_4NH_2$ structure prepared from a quenched melt suggests

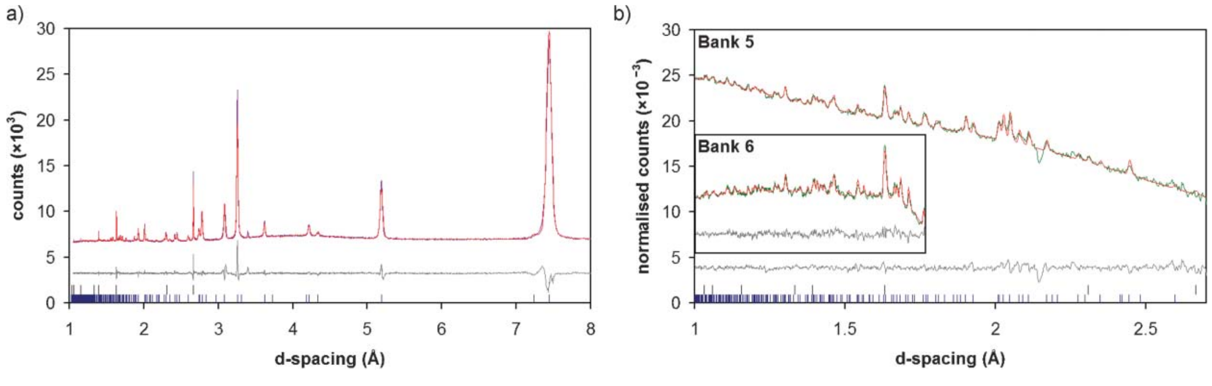

Fig. 2 Final Rietveld plots for (a) X-ray and (b) neutron diffraction data showing observed (purple and green respectively), calculated (red) and difference (grey) plots. Peak positions for $Li_2BH_4NH_2$ (blue) and Li_2O[15] (black) are indicated.

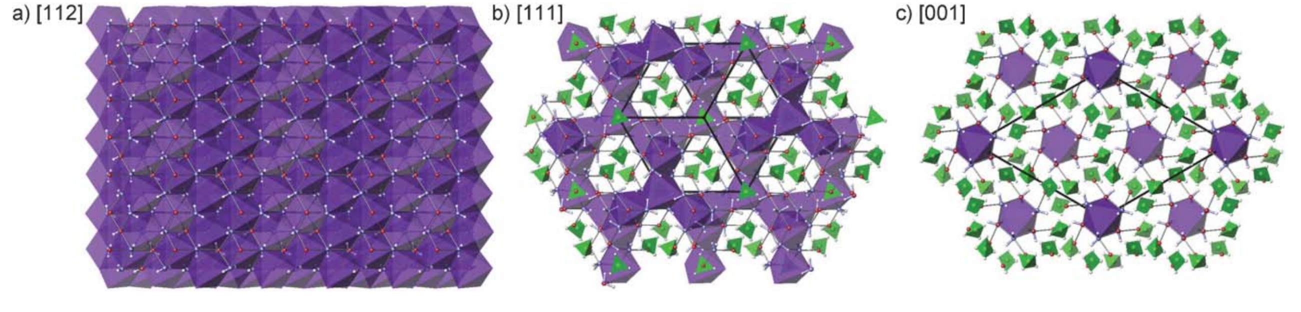

Fig. 3 Diagram showing the relationship between the N octahedra of (a) $LiNH_2$, (b) $Li_4BH_4(NH_2)_3$ and (c) $Li_2BH_4NH_2$. H atoms are depicted in white, Li in red, B in green and N in blue. NH_2^- octahedra are shown in purple.[20] The viewing directions shown are all perpendicular to the [110] direction.

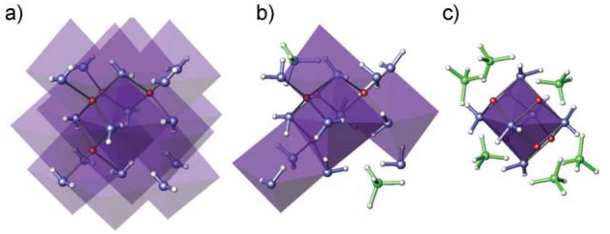

Fig. 4 Diagram showing the local structure around a single N octahedron in (a) $LiNH_2$, (b) $Li_4BH_4(NH_2)_3$ and (c) $Li_2BH_4NH_2$. H atoms are depicted in white, Li in red, B in green and N in blue. N octahedra are shown in purple.

that these units are likely to exist in the molten state, separated by the borohydride ions.

Gradual cooling of the 1 $LiBH_4$: 1 $LiNH_2$ melt at 0.5 °C min^{-1} from 190 °C resulted in $LiBH_4$ and $Li_4BH_4(NH_2)_3$ with no formation of $Li_2BH_4NH_2$. The X-ray diffraction reflections from $Li_4BH_4(NH_2)_3$ in the gradually cooled sample were very broad and a number of body centred cubic phases were observed with larger unit cell parameters. These appear to represent borohydride-rich stoichiometries that are unstable with respect to $Li_4BH_4(NH_2)_3$ and $LiBH_4$. Further annealing of this mixture at 90 °C gave only $LiBH_4$ and $Li_4BH_4(NH_2)_3$. $Li_2BH_4NH_2$ appears to be stable indefinitely at room temperature and no sign of degradation was observed in the X-ray diffraction pattern after 10 months. On heating to just below the melting point $Li_2BH_4NH_2$ decomposed to $Li_4BH_4(NH_2)_3$ and $LiBH_4$ confirming its intrinsic metastability.

Compounds containing amide anions,[21] including $Li_4BH_4(NH_2)_3$,[4–7] are currently amongst the most intensively studied as potential hydrogen storage materials. The chemical ability of borohydride ions to promote decomposition pathways in favour of H_2 rather than NH_3 release has already been demonstrated.[22] The ability of lithium borohydride, illustrated in both $Li_4BH_4(NH_2)_3$ and $Li_2BH_4NH_2$, to engineer the arrangement of NH_2^- ions at the nano-scale level combined with the low melting point of amide–borohydride mixtures and the observation that many complex hydrides desorb hydrogen from the molten state together suggest that borohydrides have a vital role in optimising the hydrogen storage properties of these materials.

We wish to thank Andy Fitch and Irene Margiolaki for assistance in using beamline ID31 at the ESRF, Grenoble, and Ron Smith and Richard Ibberson for assistance at ISIS. PAC acknowledges the EPSRC for funding.

Notes and references

1 F. E. Pinkerton, G. P. Meisner, M. S. Meyer, M. P. Balogh and M. D. Kundrat, *J. Phys. Chem. B Lett.*, 2005, **109**(1), 6.
2 M. Aoki, K. Miwa, T. Noritake, G. Kitahara, Y. Nakamori, S. Orimo and S. Towata, *Appl. Phys. A: Mater. Sci. Process.*, 2005, **80**, 1409.
3 Y. Nakamori, A. Ninomiya, G. Kitahara, M. Aoki, T. Noritake, K. Miwa, Y. Kojima and S. Orimo, *J. Power Sources*, 2006, **155**(2), 447.
4 G. P. Meisner, M. L. Scullin, M. P. Balogh, F. E. Pinkerton and M. S. Meyer, *J. Phys. Chem. B*, 2006, **110**(9), 4186.
5 Y. E. Filinchuk, K. Yvon, G. P. Meisner, F. E. Pinkerton and M. P. Balogh, *Inorg. Chem.*, 2006, **45**(4), 1433.
6 P. A. Chater, W. I. F. David, S. R. Johnson, P. P. Edwards and P. A. Anderson, *Chem. Commun.*, 2006, **23**, 2439.
7 T. Noritake, M. Aoke, S. Towata, A. Ninomiya, Y. Nakamori and S. Orimo, *Appl. Phys. A: Mater. Sci. Process.*, 2006, **83**(2), 277.
8 X-ray diffraction data were collected on the ID31 diffractometer at the ESRF, Grenoble at a wavelength of 0.80162 Å and 0.003° respectively. 372 reflections were used in the refinement. The sample was loaded into a quartz capillary in a nitrogen atmosphere glove bag and sealed with a gas torch.
9 Neutron diffraction data were collected (without isotopic enrichment) on GEM at the ISIS spallation neutron source at the Rutherford Appleton Laboratory. 421 and 364 reflections from banks 5 and 6, respectively, were used in the refinement. The sample was loaded into a vanadium can inside an argon atmosphere glove box and sealed with iridium metal wire.
10 *CRC Handbook of Chemistry and Physics*, *Internet Version 2007*, *(87th Edition)*, 〈http:/www.hbcpnetbase.com〉, ed. David R. Lide, Taylor and Francis, Boca Raton, FL, 2007.
11 A pycnometer measurement gave a sample density of 0.8703(9) g cm^{-3} which, within errors, is consistent with the calculated density for $Li_2BH_4NH_2$ with a *ca.* 5.7% Li_2O impurity. See reference 15.
12 A. A. Coelho, *TOPAS, General Profile and Structure Analysis Software for Powder Diffraction Data*, version 3.0; Bruker AXS: Karlsruhe, Germany, 2004.
13 See Electronic Supplementary Information for pictorial representations of these structures†.
14 A. C. Larson and R. B. Von Dreele, *General Structure Analysis System (GSAS)*, Los Alamos National Laboratory Report LAUR 86–748 (2000).
15 Li_2O present from the $LiNH_2$ starting material was also observed at *ca.* 5.7%.
16 M. Nagib and H. Jacobs, *Atomkernenergie*, 1973, **21**(4), 275.
17 M. Nagib, H. Kistrup and H. Jacobs, *Atomkernenergie*, 1975, **26**(2), 87.
18 H. Jacobs and B. Harbrecht, *J. Less-Common Met.*, 1982, **85**(1), 87.
19 H. Jacobs, *Z. Anorg. Allg. Chem.*, 1971, **382**(2), 97.
20 See Electronic Supplementary Information for animated version of Fig. 3†.
21 H. Y. Leng, T. Ichikawa, S. Hino, N. Hanada, S. Isobe and H. Fujii, *J. Phys. Chem. B*, 2004, **108**(26), 8763; Y. Nakamori, G. Kitahara and S. Orimo, *J. Power Sources*, 2004, **138**(1–2), 309; J. Lu and Z. Z. Fang, *J. Phys. Chem. B*, 2005, **109**(44), 20830; J. Lu, Z. Z. Fang and H. Y. Sohn, *J. Phys. Chem. B*, 2006, **110**(29), 14236; R. Janot, J.-B. Eymery and J.-M. Tarascon, *J. Phys. Chem. C*, 2007, **111**(5), 2335.
22 P. A. Chater, P. A. Anderson, J. W. Prendergast, A. Walton, V. S. J. Mann, D. Book and W. I. F. David, *J. Alloys Compd.*, 2007, **446–447**, 350.